Free Rad. Res. Comms., Vols. 12-13, pp. 259-268
Reprints available directly from the publisher
Photocopying permitted by license only

STRUCTURE-FUNCTION RELATIONSHIPS IN IRON AND MANGANESE SUPEROXIDE DISMUTASES

WILLIAM C. STALLINGS,[1] ANITA L. METZGER,[2] KATHERINE A. PATTRIDGE,[2] JAMES A. FEE,[3] and MARTHA L. LUDWIG[2+]

Biophysics Research Division and Department of Biological Chemistry, University of Michigan[2] and Isotope and Nuclear Chemistry Division, Los Alamos National Laboratory[3], USA

Using the complete sequences for MnSOD from *Thermus thermophilus* and for FeSOD from *E. coli*, structural models for both oxidized enzymes have been refined, the Mn protein to an *R* of 0.186 for all data between 10.0 and 1.8 Å, and the Fe protein to an *R* of 0.22 for data between 10.0 and 2.5 Å. The results of the refinements support the presence of a solvent as a fifth ligand to Mn(III) and Fe(III) and a coordination geometry that is close to trigonal bipyramidal. The putative substrate-entry channel is comprised of residues from both subunits of the dimer; several basic residues that are conserved may facilitate approach of O_2^-, while other conserved residues maintain interchain packing interactions. Analysis of the azide complex of Fe(III) dismutase suggests that during turnover O_2^- binds to the metal at a sixth coordination site without displacing the solvent ligand. Because crystals reduced with dithionite show no evidence for displacement of the protein ligands, the redox-linked proton acceptor (C. Bull and J.A. Fee (1985), *Journal of the American Chemistry Society* **107**, 3295-3304) is unlikely to be one of the histidines which bind the metal ion. Structural, kinetic, titration, and spectroscopic data can be accommodated in a mechanistic scheme which accounts for the differential titration behaviour of the Fe(III) and Fe(II) enzymes at neutral and high pH.

KEY WORDS: x-ray structure, substrate path, invariant residues, pKs, redox-linked pKs, azide complex.

INTRODUCTION

The Fe and Mn superoxide dismutases possess a characteristic dimeric structure in which residues from both chains contribute to substrate binding and to formation of the metal binding site.[1-4] Crystallographic refinement of the structures of *E. coli* FeSOD[1,5] and *T. thermophilus* MnSOD,[3] using the sequences that have been determined recently,[5,6] permits us to analyze the geometry of the metal binding sites and to present in detail the features of the pathway which superoxide presumbly follows to reach the metal site. Structural studies of the Mn(II) form of *T. thermophilus* dismutase and of the binding of azide to Fe(III)SOD have added significantly to information about intermediates in the catalytic cycle. Finally, comparisons based on the three-dimensional structures, along with alignment of a number of sequences,

[1] Present address: Physical Sciences Center, Monsanto, BB4K 700 Chesterfield Village Parkway, St. Louis 63198, MO, USA.
[+] Corresponding author.

suggest roles for several conserved residues that are not in the immediate vicinity of the active site.

RESULTS AND DISCUSSION

The Metal Center in the Oxidized Enzymes

The positions of the metal ligands in MnSOD from *T. thermophilus*, after refinement

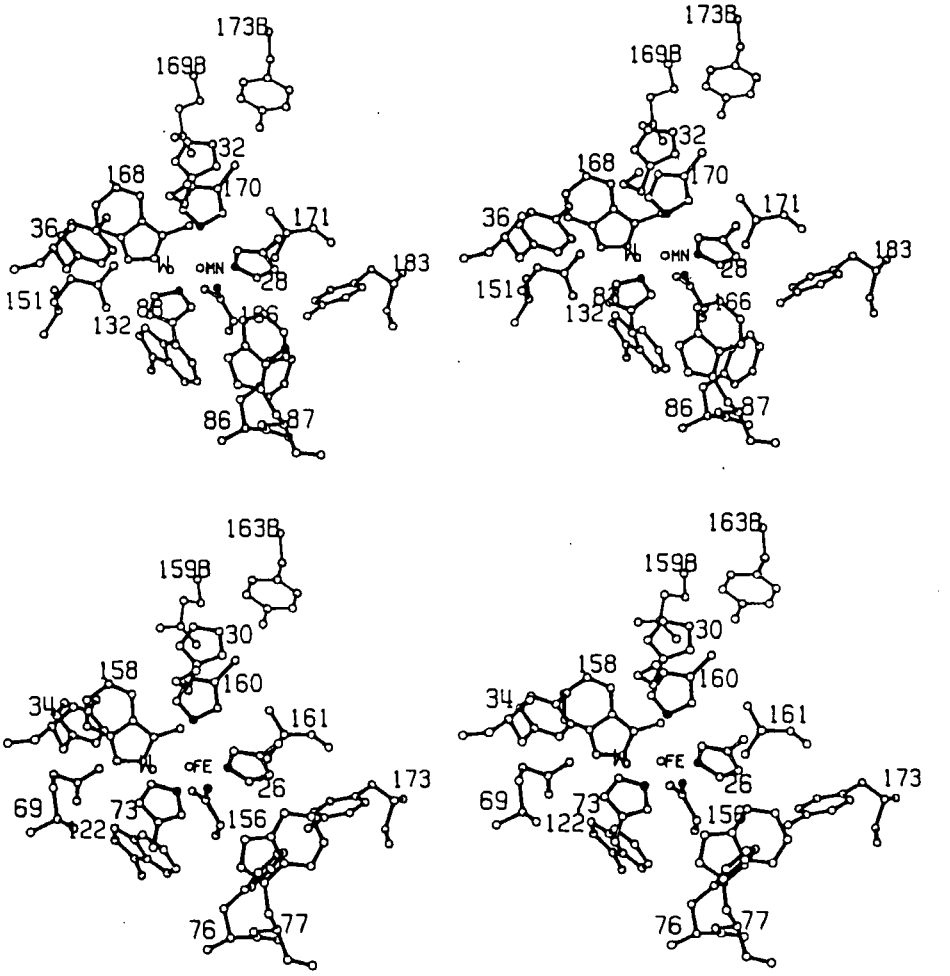

FIGURE 1 Top. The active center of Mn superoxide dismutase from *T. thermophilus*. The side chains that bind the metal are shown with open bonds and the protein atoms bonded to Mn are filled. The five ligand atoms lie approximately at the vertices of a trigonal bipyramid. Coordinates for this drawing are from a refined model including 187 solvents, with $R = 0.186$ for all data between 1.8 and 10 Å. Restraints applied during refinement[8] included repulsive interactions to prevent the ligand-metal distances from becoming too small, but did not include any terms involving angles at the metal ion. Bottom. The active center of Fe superoxide dismutase from *E. coli* in the same orientation and notation as in the top panel. Coordinates are from XPLOR[9] refinement with data from 10.0 to 2.5 Å and $R = 0.22$. Gln 69 in Fe dismutase forms the same interactions as Gln 151 in MnSOD.

bacterial dismutases (Figure 1). The arrangement of the ligands is best represented by a trigonal bipyramid, since the bond angle at Mn for the axial ligands, NE2 of His 28 and O of solvent, is 175° and the bonds between the axial ligands and Mn are nearly perpendicular (85–95°) to the plane formed by the remaining three ligands. The metal ion is displaced only 0.15 Å from the plane formed by 166 OD1, 83 NE2 and 170 NE2; the most obvious distortions from an ideal trigonal bipyramid are found among the angles in the trigonal plane, with N–Mn–N approximately 130°. The occupancy and thermal parameters of the axial solvent ligand to Mn have been refined to values of 0.99 and 8.0 $Å^2$ (average of the A and B chain); average parameters for the Mn(III) ion are 1.00 and 10.4 $Å^2$. Thus the metal sites are fully occupied in each monomer chain. Our findings for *T. thermophilus* MnSOD differ from those of Parker and Blake,[4] who assigned partial occupancy to the metal sites in *B. stearothermophilus* MnSOD and found no density corresponding to a water ligand, although the coordination geometry otherwise resembles that found in the *T. thermophilus* enzyme. Extension of the resolution of *E. coli* FeSOD is still in progress, with R currently 0.22 for data between 10.0 and 2.5 Å, and the occupancy at the solvent ligand site has not yet been refined. However, a distinctive peak appears at the water position in difference maps whenever this ligand is omitted from structure factor calculations.

The residues surrounding the metal-ligand cluster are shown for both MnSOD and FeSOD in Figure 1. The hydrophobicity of this 'second shell' of residues has been emphasized in several discussions,[3,7] as has the participation of residues from both chains of the dimer unit. Here we would like to comment on the distribution of charge in the active center. In the oxidized enzymes the formal charge on the central metal is +3. Such a large positive charge in a low dielectric environment is likely to be compensated by corresponding negative charges. At neutral pH one would expect the Asp 166 ligand to be present in the COO^- form, reducing the formal charge of the ligand cluster to +2. Further partial compensation may be provided by Glu 169B (at 7 Å from Mn A) but if the histidines and tyrosines display their normal pKs, they will be uncharged (see below), leaving a significant net positive charge on the metal-ligand cluster at neutral pH. For this reason we suggest that the solvent ligand in the oxidized enzymes is OH^- rather than H_2O.

Binding of Inhibitors and Substrates

The packing of residues next to histidines 73 and 160 in FeSOD or histidines 83 and 170 in MnSOD is imperfect, leaving a vacancy or hole that does not appear to be occupied by a solvent molecule (Figure 2). This region, bounded on its other sides by His 30, His 31 and Tyr 34 in FeSOD, corresponds to the location of positive density in difference maps comparing the structures of Fe(III)SOD and its azide complex. At 2.5 to 3.0 Å resolution, the major positive feature in these maps can be fit by a linear N_3^- with the terminal nitrogen about 2.0 Å from the Fe^{+3} ion and an iron-azide bond angle near 120° (Figure 2). The ligated azide nitrogen is approximately coplanar with the ligand atoms from His 73, His 160 and Asp 156. In these studies at moderate resolution, positive and negative peaks ajoining the rings of histidines 73 and 160 suggest ligand shifts that change the coordination geometry to accommodate azide binding. Our interpretation is that azide binds to Fe(III) without displacement of the solvent ligand, increasing the coordination number to six. We propose that superoxide anion and the reaction products bind like azide and that during turnover the metal cycles between 5- and 6-coordinate species.

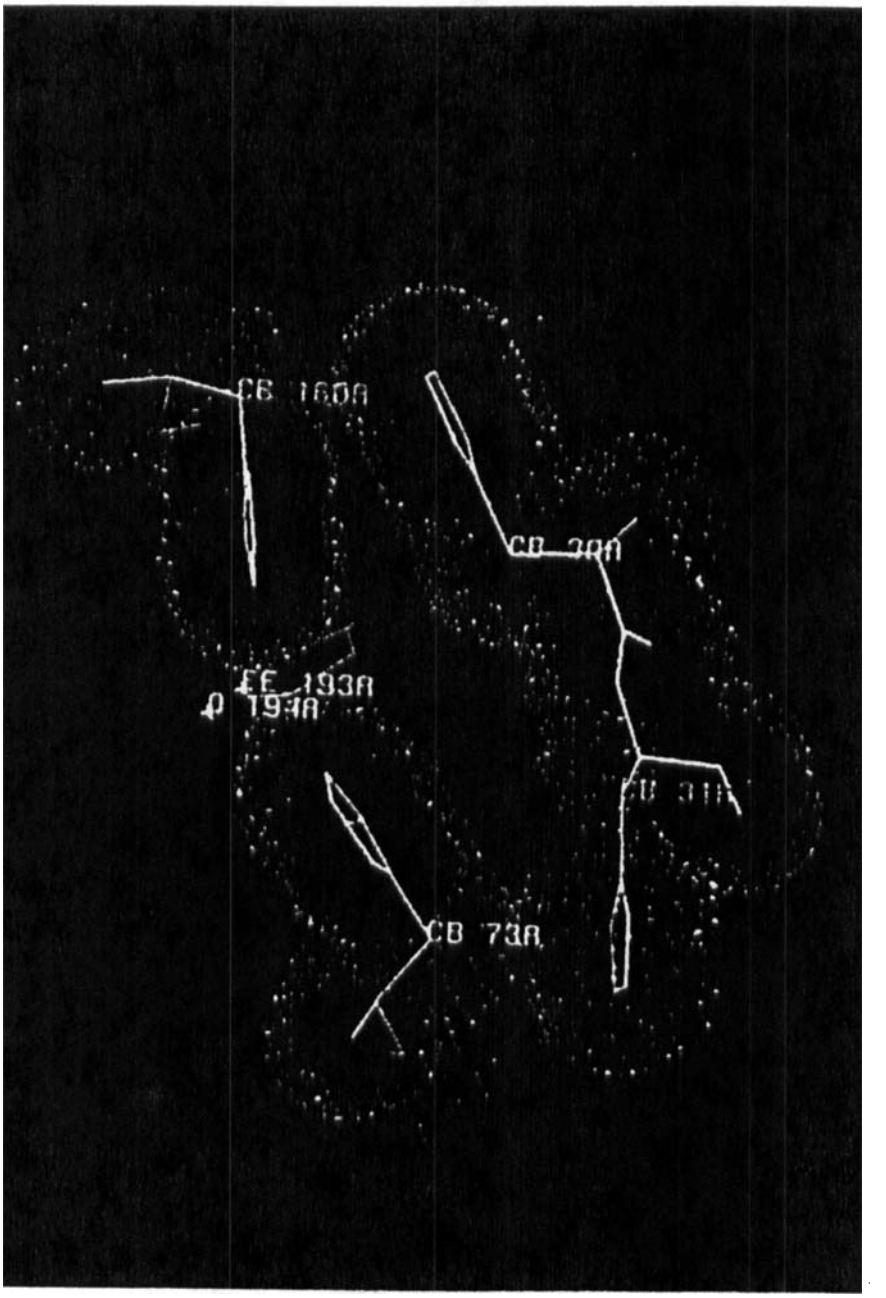

FIGURE 2 A. A slab through the atomic model of Fe(III)SOD showing the cavity formed between the metal ligands, His 73 and His 160, and residues His 30 and His 31. Dot surfaces are drawn at van der Waals radii. Tyr 34, not shown in this view, partly obscures entry to the cavity.

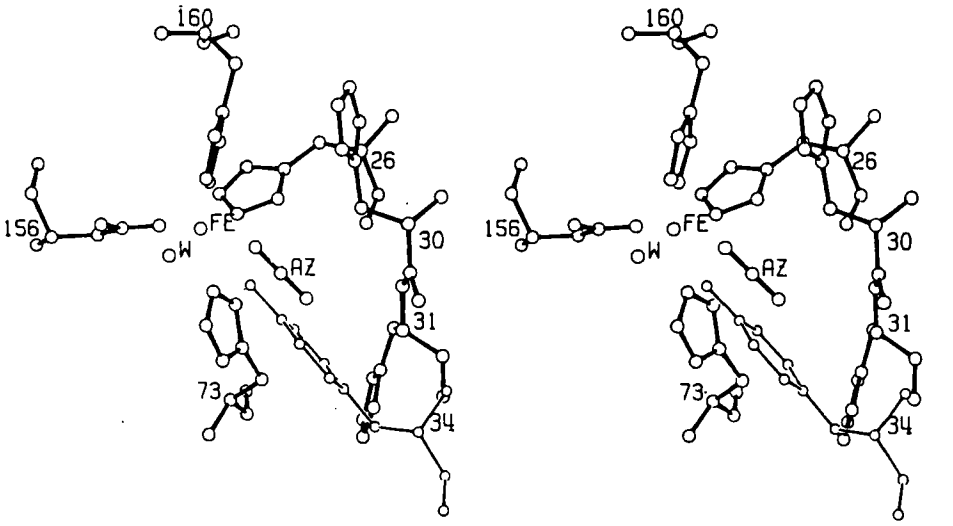

FIGURE 2 B. A model of azide bound to Fe(III)SOD, depicted in approximately the same orientation as panel A and showing the metal coordinated to six ligands. A linear N_3^- has been built into different density observed in maps with coefficients $(|F_{az}| - |F_{nat}|)\exp(ia_{nat})$ at 2.5 Å resolution. Positions of histidines 73 and 160 have been adjusted to fit densities in maps resulting from refinement of data from the Fe(III)SOD azide complex at 2.5 Å resolution.

Access of Substrate and Inhibitors to the Metal Site

Inspection of the structures suggests that the pathway from bulk solution to the catalytic site is a funnel or channel lined with solvents that interact with main chain and side chain atoms from each monomer of the fundamental dimeric unit found in all Fe and Mn dismutases. The outermost entry of the channel in MnSOD is formed from Arg 180 and Met 125 of the B chain, along with Asn 39, Asn 75 and Asn 76 of the A chain (Figure 3). Moving inward toward the metal, the next layer of side chains includes Lys 31A, Phe 128B, Tyr 172B and Asn 178B. The innermost residues are His 32A, Tyr 36A, Glu 169B and Tyr 173B.

Displays of van der Waals surfaces or of accessible surfaces[10] demonstrate that residues 32 and 36 prevent access of a water molecule to the space bounded by the rings of histidines 83 and 170, suggesting that inner sphere interactions of superoxide or other ligands with the metal require the transient opening of the gate formed by His 32 and Tyr 36. Simulations of the reaction of superoxide with Fe or Mn dismutases[11] confirm the inaccessibility of the metal site in the static structures.

Residues in the funnel may serve dual roles, both facilitating entry of substrate and stabilizing the dimer interface. It is not surprising that many are invariant or semi-invariant (Figure 4). In particular, basic residues at the outer positions that are 180B and 31A in MnSOD may assist substrate approach to the metal site. Chemical modification of Arg[12] or Lys[12,13] impairs the catalytic activity of manganese or iron enzymes from *E. coli*. Deeper in the channel, His 32, buttressed by Tyr 173B, may also furnish a positive charge to attract anions. Arg 180B contacts only B chain residues and may be replaced by Lys, as in yeast MnSOD; the residue which packs against it,

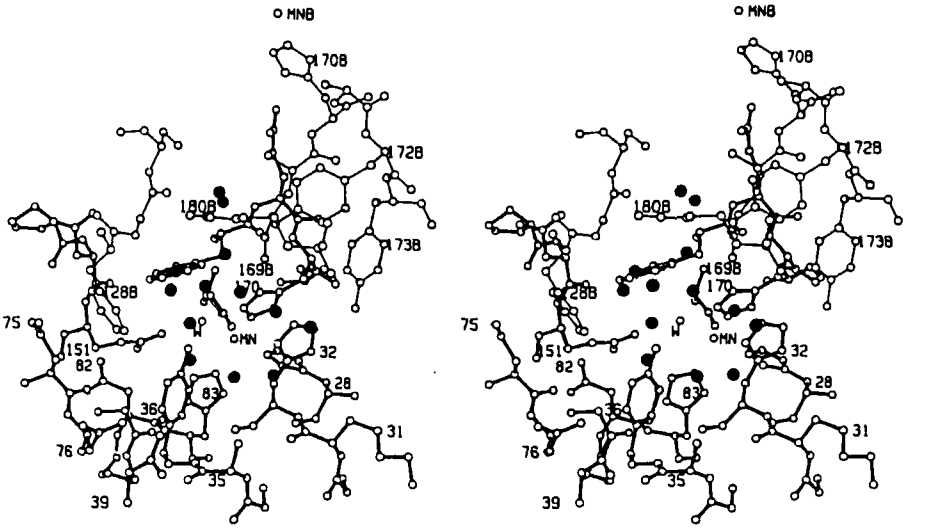

FIGURE 3 A view of the solvent-lined channel or mouth that connects the metal-ligand center with bulk solvent in MnSOD. It is presumed that the substrate takes a path approximately perpendicular to this view. The channel waters are represented as filled spheres somewhat larger than the protein atoms. Midway down, His 32 and Tyr 36 must be passed by ligands that form inner sphere complexes. Each monomer chain forms one of the lips at the mouth of the channel. Residues from the second, or "B", chain of the dimer are drawn with thinner bonds; those from the primary "A" chain are drawn with thicker bonds. The Mn ion and one of its ligands in the B chain have been included to show the relationship between the two active centers. A number of main and side chain atoms have been omitted from the drawing; e.g. His 33 has been removed, as has the side chain at 34, and waters other than those occupying the channel are not shown. Met 125B packs against Arg 180B and partly shields the guanidinium group, but has not been included in this picture.

Met 124B in *T. thermophilus* MnSOD, is variable but apolar. Lys 31 and His 32, more highly conserved, contribute to the A–B chain interactions as well as to formation of the substrate channel. An interesting semiconservative pairing occurs between Phe 128B, which protrudes into the substrate channel of the A chain, and Asn 75A. These residues stack against each other to make part of the A:B chain interface. In yeast and human MnSODs, these residues are Gln in the B chain and Phe in the A chain, substitutions which can preserve the interchain stacking interaction. Both Glu 169B and Tyr 173B penetrate across the dimer interface to form hydrogen bonds with active center residues of the A chain and are conserved although they may not come into direct contact with substrate.

Titration of Groups in the Metal Binding Site: Comparison of Me(III) and Me(II) Structures

Several observations suggest that groups on or near the metal undergo ionization in the pH range 5 to 11. Visible and epr spectra of Fe(III)SOD indicate a reversible ionization with $pK_a \sim 5$ and spectral, anion binding, and kinetic experiments establish an ionization with $pK_a \sim 9$ in the oxidized protein.[19] Kinetic observations have also suggested an ionization in the reduced form of the protein, having a $pK \sim 9$.[20] Further, Bull and Fee[20] demonstrated that reduction of the metal ion is linked to the

Manganese Dismutases			
T. thermophilus	^{74}R-N-N-G-G-G-H-L-N-H-S	^{125}M-G-R-F-G-S-G-W	^{177}Q-M-R-R-A
B. stearothermophilus	^{72}R-N-N-G-G-G-H-A-N-H-S	^{123}A-G-R-F-G-S-G-W	^{174}Q-N-R-R-P
E. coli B	^{72}R-N-N-A-G-G-H-A-N-H-S	^{121}A-S-R-F-G-S-G-W	^{178}Q-N-R-R-P
Yeast	^{72}K-F-H-G-G-G-F-T-N-H-C	^{126}A-G-V-Q-G-S-G-W	^{179}Q-N-K-K-A
Human liver	^{65}K-F-N-G-G-G-H-I-N-H-S	^{116}V-G-V-Q-G-S-G-W	^{168}K-N-V-R-P
Iron Dismutases			
E. coli K12	^{64}F-N-N-A-A-Q-V-W-N-H-T	^{115}I-K-N-F-G-S-G-W	^{167}R-N-A-R-P
Ph. leiognathi	^{64}F-N-N-A-A-Q-V-W-N-H-T	^{115}I-K-N-F-G-S-G-W	^{168}R-N-L-R-P

FIGURE 4 Sequences (5,6,14–18) that contribute residues to the channel depicted in Figure 3. Alignments are taken from the references describing the sequences, and are consistent with comparisons of the three dimensional structures.[1,3,4] Conservation of sequences spanning the metal ligands has been discussed.[3,24] The alignments shown here illustrate conservation of basic residues at positions 31 and 180 and of interchain packing and hydrogen bonding involving residues 75 and 128 (*T. thermophilus* MnSOD numbering).

uptake of one proton per electron throughout the pH range of 7.0 to 10.0 in which they conducted the measurements. In order to account for for these data, a highly basic group ($pK > 11$) must be formed on adding an electron to the Fe(III) form of the protein, and an acidic group ($pK < 6$) must be formed on removing an electron from the Fe(II) form of the protein. Moreover, the pK of 9.0 associated with hydrolysis of Fe(III) must be compensated by a new pK of 9.0 in the reduced enzyme.[20] Because pKs of ligands are so strongly influenced by the charge of the metal, attempts to identify ionizing groups have focussed initially on the imidazole and solvent ligands to the metal ion.

Conceivably, one of the imidazole ligands could serve as the redox-linked proton acceptor. However, protonation of a neutral histidine ligated to Fe or Mn would be expected to displace the imidazole ring from the metal and should therefore be detectable in the structures of the reduced enzymes as a shift in the ring position. X-ray data have been collected from crystals of dithionite-reduced MnSOD (pH 7.0) to a resolution of 2.4 Å and subjected to crystallographic refinement[8] with the five metal ligands omitted from the atomic model to avoid bias toward the ligand positions found in the Mn(III) structure. After refinement to an R of 0.200 (129 solvents) for data between 5.0 and 2.3 Å, ($|F_{obs}| - |F_{calc}|$) difference maps display densities that correspond closely to the ligand positions of the oxidized MnSOD structure. The Fe(III) and Fe(II)SOD structures have been compared at lower resolution (4 Å); difference maps show no features suggesting dissociation of one of the histidine ligands. Our observations on the Fe enzymes are consistent with Solomon's conclusion from MCD measurements that Fe(II)SOD is 5-coordinate.[21] Results of our studies of both Fe(II)SOD and Mn(II)SOD are incompatible with the proposal that an uncharged His ligand is the redox-linked proton acceptor.

In Cu/Zn dismutase, His 61, the residue bridging the two metals, is anionic and does act as a proton acceptor, with the resulting neutral imidazole dissociating from Cu^{+1}.[22] Imidazolate 61 in the Cu/Zn enzyme is in a very different environment from any of the His ligands in the Fe or Mn enzymes, and it seems unlikely that one of the

His residues might exist in the anionic form in the oxidized Mn or Fe enzymes. The ND1 atoms of histidines 83 and 170 in MnSOD are 2.6 and 2.8 Å from carbonyl oxygen 79 and the carboxyl oxygen of Glu 169B, respectively, indicating that these histidines exist as uncharged species with hydrogen at ND1, and ND1 of His 28 is 2.65 Å from a trapped solvent.

We would like to present a new idea which appears to account for the high pH ionizations observed in both Fe(III) and Fe(II) species. At neutral pH, Fe(III) is postulated to coordinate an OH^- ion rather than the H_2O previously hypothesized.[20] Fe(II) is postulated to coordinate H_2O at neutral pH and to resist hydrolysis even at pH 11. That hydrolysis does not occur below this pH is based on Mössbauer studies of the reduced enzyme at pH 7 and pH 10.8.[23] The Mössbauer spectra from samples at these two pHs are typical of high spin Fe(II) and are essentially superimposable. If a water molecule bound to the Fe(II) at pH 7 hydrolyzed to OH^- below pH 10.8, the parameters of the Mössbauer spectrum would be significantly changed. Thus a coordinated water is not the ionizing group affecting the kinetic properties of the Fe(II) enzyme. In addition, the Mössbauer spectra indicate that the Fe(II) enzyme is not further hydrated at high pH and therefore remains pentacoordinate. An important aspect of scheme I is that at least two groups are responsible for the differential

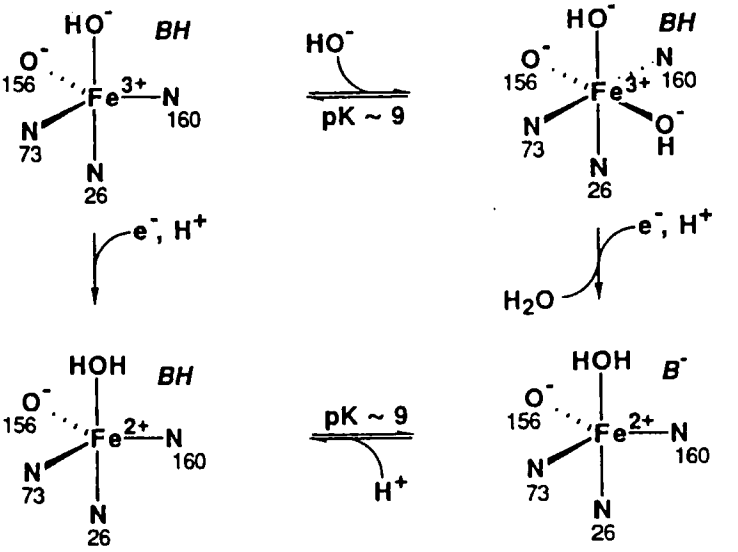

Scheme I

titration behavior of the Fe(III) and Fe(II) enzymes. In Ref. 20, the group accepting a proton on reduction at neutral pH was assumed to be a ligand, charge type unstipulated, that also titrated at pH 9 in the reduced enzyme. The new X-ray and Mössbauer data lead us to introduce an alternative scheme in which a non-ligand group, here denoted BH, is sufficiently near the Fe to stabilize the high pH form of the oxidized protein.

The *pKs* and the H^+/e^- data are accounted for as follows. In analogy with the crystallographically observed binding of azide, the *pK* of 9.0[19] that is signalled by

spectral changes in Fe(III)SOD corresponds to the addition of OH^- at the sixth ligand position; the formal charge on the metal complex would then be 0. At high pH the protein group BH is presumed to interact with and stabilize $Fe(III)(OH^-)_2$ in its BH form. In the reduced protein, the $pK \sim 9$ corresponds to ionization of BH. The resulting B^- does not affect the electric field gradient at the iron, as demanded by the Mössbauer data, but its presence could affect the rate of binding of O_2^- to the reduced protein.[20] Reduction of the protein at high pH is accompanied by binding of one proton to each of the OH^- ligands, loss of a coordinated water (as required by the Mössbauer data) and ionization of BH. This results in a net $H^+/e^- = 1$, as required by the titration data. On reduction of the enzyme at neutral pH, the OH^- ligand would accept a proton.

There is some support for this scheme in the crystallographic data. Difference Fourier maps of MnSOD, based on amplitudes ($|F_{ox}| - |F_{red}|$) for data between 8.0 and 2.4 Å and phases computed from the most accurate model for Mn(III)SOD, show very few changes accompanying reduction, as expected from the refinement results described earlier. However, the strongest peaks are positive and negative features on either side of the water ligand, suggesting a small displacement of the metal-bound solvent oxygen toward the 'free' O of Asp 166 which might be expected on protonation of an OH^- ligand. Tyrosine 36 in MnSOD, or Tyr 34 in FeSOD, lies in close proximity to the metal and is conserved in the known Fe- and MnSOD sequences;[24] in our current models, the phenolic oxygen of Tyr 34 is about 3.5 Å from the azide nitrogen that binds to Fe(III). It has been suggested previously[3,4,7] that this residue may be associated with the ionization properties of the metal center in SODs. Here we propose that Tyr 34 in FeSOD may be the residue which stabilizes the high pH form of the oxidized enzyme as ROH but ionizes to RO^- at pH 9.0 in the Fe(II) enzyme. Site mutagenesis experiments in progress may test the validity of this proposal.

Acknowledgements

This research was supported by grants from the National Institutes of Health (GM 16429 and RR 02451 to MLL and GM 35189 to JAF), and from the National Science Foundation (PCM 8401634 to MLL). Some of the x-ray data were measured at the Multiwire Area Detector Facility at the University of California, San Diego, which is supported by NIH-RR 01644. Crystallographic refinements were carried out at the San Diego Supercomputer Center, and XPLOR calculations conducted at the Monsanto Cray-XMP. We thank Drs. Christopher Bull and Eric Niederhoffer for helpful discussions and comments.

References

1. W.C. Stallings, T.B. Powers, K.A. Pattridge, J.A. Fee and M.L. Ludwig (1983) Iron superoxide dismutase from *Escherichia coli* at 3.1 Å resolution. *Proceedings of the National Academy of Sciences, USA*, **80**, 3884–3888.
2. D. Ringe, G.A. Petsko, F. Yamakura, K. Suzuki and D. Ohmori (1983) Structure of iron superoxide dismutase from *Pseudomonas ovalis* at 2.9 Å resolution. *Proceedings of the National Academy of Sciences USA*, **80**, 3897–3883.
3. W.C. Stallings, K.A. Pattridge, R.K. Strong and M.L. Ludwig (1985) The structure of manganese superoxide dismutase from *Thermus thermophilus HB8* at 2.4 Å resolution. *Journal of Biological Chemistry*, **260**, 16424–16432.
4. M.W. Parker and C.F. Blake (1988) Crystal structure of manganese superoxide dismutase from *Bacillus stearothermophilus* at 2.4 Å resolution. *Journal of Molecular Biology*, **199**, 649–661.
5. A. Carlioz, M.L. Ludwig, W.C. Stallings, J.A. Fee, H.M. Steinman and D. Touati (1988) Iron superoxide dismutase. Nucleotide sequence of the gene from *Escherichia coli K12* and correlations

with crystal structures. *Journal of Biological Chemistry*, **263**, 1555–1562.
6. S. Sato, Y. Nakada and K. Nakasawa-Tomizawa (1987) Amino-acid sequence of a tetrameric manganese superoxide dismutase from *Thermus thermophilus HB. Biochimica et Biophysica Acta*, **912**, 178–184.
7. M.L. Ludwig, K.A. Pattridge and W.C. Stallings (1986) Manganese superoxide dismutase. In *Manganese in Metabolism and Enzyme Function* (eds. V.L. Schramm and F.C. Wedler) Academic Press, 405–430.
8. W.A. Hendrickson (1985) Stereochemically restrained refinement of macromolecular structures. *Methods in Enzymology*, **115**, 252–270.
9. A.T. Brünger, M. Karplus, and G.A. Petsko (1989) Crystallographic refinement by simulated annealing: application to crambin. *Acta Crystallographica*, **A45**, 50–61.
10. F.M. Richards (1985) Calculation of molecular volumes and areas for structures of known geometry. *Methods in Enzymology*, **115**, 440–464.
11. J. Sines, S. Allison, A. Wierzbicki and J.A. McCammon. Brownian dynamics simulation of the superoxide-superoxide dismutase reaction: Fe and Mn enzymes. *Journal of Physical Chemistry*, in press.
12. C.L. Borders, Jr., P.J. Horton and W.F. Beyer, Jr. (1989) Chemical modification of iron- and manganese-containing superoxide dismutases from *Escherichia coli*. *Archives of Biochemistry and Biophysics*, **268**, 74–80.
13. J. Benkovic, T. Tillman, A. Cudd and I. Fridovich (1983) Electrostatic facilitation of the reaction catalyzed by the manganese-containing and iron-containing superoxide dismutases. *Archives of Biochemistry and Biophysics*, **221**, 329–332.
14. C.J. Brock and J.E. Walker (1980) Superoxide dismutase from *Bacillus stearothermophilus*. Complete amino acid sequence of a manganese enzyme. *Biochemistry*, **19**, 2873–2882.
15. H.M. Steinman (1978) The amino acid sequence of manganese superoxide dismutase from *Escherichia coli B*. *Journal of Biological Chemistry*, **253**, 8708–8720.
16. C. Ditlow, J.T. Johansen, B.M. Martin and I. Svendsen (1982) The complete amino acid sequence of manganese superoxide dismutase from *Saccharomyces cerevisiae*. *Carlsberg Research Communications*, **47**, 81–91.
17. D. Barra, M.E. Schinina, M. Simmaco, J.V. Bannister, W.H. Bannister, G. Rotilio and F. Bossa (1984) The primary structure of human liver manganese superoxide dismutase. *Journal of Biological Chemistry*, **259**, 12595–12601.
18. D. Barra, M.E. Schinina, W.H. Bannister, J.V. Bannister, and F. Bossa (1987) The primary structure of iron-superoxide dismutase from *Photobacterium leiognathi*. *Journal of Biological Chemistry*, **262**, 1001–1009.
19. J.A. Fee, G.J. McClune, A.C. Lees, R. Zidovetski and I. Pecht (1981) The pH dependence of the spectral and anion binding properties of iron containing superoxide dismutase from *E. coli B*: an explanation for the azide inhibition of dismutase activity. *Israel Journal of Chemistry*, **21**, 54–58.
20. C. Bull and J.A. Fee (1985) Steady-state kinetic studies of superoxide dismutases: properties of the iron containing protein from *Escherichia coli*. *Journal of the American Chemistry Society*, **107**, 3295–3304.
21. J.W. Whittaker and E.I. Solomon (1986) Spectroscopic studies on ferrous non-heme iron active sites: variable-temperature MCD probe of ground- and excited-state splittings in iron superoxide dismutase and lipoxygenase. *Journal of the American Chemistry Society*, **108**, 835–836.
22. I. Bertini, C. Luchinat and R. Monnanni (1985) Evidence of the breaking of the copper-imidazolate bridge in copper/cobalt-substituted superoxide dismutase upon reduction of the copper (II) centers. *Journal of the American Chemistry Society*, **107**, 2178–2179.
23. E.C. Niederhoffer, J.A. Fee, V. Papaefthymiou and E. Münck (1987) Magnetic resonance studies involving iron superoxide dismutase from *E. coli*. *Isotope and Nuclear Chemistry Division, Annual Report, Los Alamos National Laboratory*, 79–84.
24. M.W. Parker, M.E. Schinina, F. Bossa and J.V. Bannister (1984) Chemical aspects of the structure, function, and evolution of superoxide dismutases. *Inorganica Chimica Acta*, **91**, 307–317.

Accepted by Prof. G. Czapski